Relationship Between Task-Related Gamma Oscillations and BOLD Signal: New Insights From Combined fMRI and Intracranial EEG

Jean-Philippe Lachaux,[1]* Pierre Fonlupt,[1] Philippe Kahane,[2,3] Lorella Minotti,[2,3] Dominique Hoffmann,[4,5] Olivier Bertrand,[1] and Monica Baciu[6]

[1]*INSERM U821—Brain Dynamics and Cognition, Lyon, France*
[2]*Department of Neurology, Grenoble Hospital, Grenoble, France*
[3]*INSERM JE2413, Grenoble, France*
[4]*Department of Neurosurgery, Grenoble Hospital, Grenoble, France*
[5]*INSERM 318, Grenoble, France*
[6]*CNRS UMR 5105, Laboratoire de Psychologie et Neurocognition, Université Pierre Mendès-France, Grenoble, France*

Abstract: Cognitive neuroscience relies on two sets of techniques to map the neural networks underlying cognition in humans: recordings of either regional metabolic changes (fMRI or PET) or fluctuations in the neural electromagnetic fields (EEG and MEG). Despite major advances in the last few years, an explicit linkage between the two is still missing and the neuroimaging community faces two complementary but unrelated sets of functional descriptions of the human brain. Such an explicit framework, linking the two approaches in potentially complex cognitive tasks and in a variety of brain regions would permit to combine them into fine spatio-temporally-grained human brain mapping procedures. We combined fMRI and intra-cranial EEG recordings of the same epileptic patients during a semantic decision task and found a close spatial correspondence between regions of fMRI activations and recording sites showing EEG energy modulations in the gamma range (>40 Hz). Our findings further support previous findings that gamma band modulations co-localize with BOLD variations and also indicate that fMRI may be used as a constraint to improve source reconstruction of gamma band EEG responses. *Hum Brain Mapp 28:1368–1375, 2007.*

Key words: fMRI; EEG; gamma band; reading

INTRODUCTION

fMRI—high spatial but poor temporal resolution—and EEG—poor spatial but high temporal resolution—are in principle complementary by nature. Though fusing the two techniques is highly desirable, it is no trivial task. The activity of a small neural population during a time window of the order of seconds is measured by fMRI as a couple of haemodynamic values and by EEG as a composite signal with a complex organization in time and frequency. Indeed, the electrophysiological response evoked by a sensory stimulation, or a motor output always takes

This article contains supplementary material available via the Internet at http://www.interscience.wiley.com/jpages/1065-9471/suppmat

*Correspondence to: Jean-Philippe Lachaux, Mental Processes and Brain Activation, INSERM—Unité 280, Centre Hospitalier Le Vinatier, Bâtiment 452, 95 Boulevard Pinel, Bron 69500, France. E-mail: lachaux@lyon.inserm.fr

Received for publication 13 July 2006; Revision 31 October 2006; Accepted 1 November 2006

DOI: 10.1002/hbm.20352

Published online 1 February 2007 in Wiley InterScience (www.interscience.wiley.com).

the form of an organised collection of event-related potentials as well as synchronizations and desynchronizations in several frequency bands including theta (4–7 Hz), alpha (8–12 Hz), beta (15–30 Hz) and gamma ranges (>40 Hz). In fact, a number of studies have demonstrated that components of EEG responses often have different spatial and temporal organisation, as well as presenting different reactivity to modulations in a subject's cognitive activity [Crone et al., 1998a,b; Foucher et al., 2003; Lachaux et al., 2005], strongly suggesting that they reflect different neural mechanisms and functions. It remains still unclear which (or which combinations) of these components has the strongest influence on the BOLD signal and this seriously limits the functional interpretation of fMRI signals.

Most of our current knowledge about the electrophysiological correlates of the BOLD signal come from recent animals studies combining simultaneous haemodynamic and spikes/local field potentials measurements [Kayser et al., 2004; Kim et al., 2004; Logothetis et al., 2001; Niessing et al., 2005]. Those studies have all shown a close correspondence between the BOLD signal and the gamma band component of the LFP, in both monkey and cat visual cortex.

This constitutes a good reason to pay specially close attention to the gamma band; others include (a) the putative role of gamma band synchronization in neural communication [Fries, 2005; Varela et al., 2001], strongly supported by numerous microelectrodes animal studies [Singer, 1999]; (b) the repeated observation, in human intracranial EEG studies, that several perceptual, motor and cognitive processes are accompanied by focal energy increases in the gamma band, matching quite precisely in their anatomical organisation the networks implicated in the same processes by fMRI studies (e.g., motor programming [Aoki et al., 2001; Crone et al., 1998a; Lachaux et al., 2006; Szurhaj et al., 2005], memory [Fell et al., 2001; Howard et al., 2003; Mainy et al., in press] or visual perception [Klopp et al., 1999; Lachaux et al., 2000, 2005; Tallon-Baudry et al., 2001, 2005; Tanji et al., 2005]). Using the same experimental attentional paradigm in intracranial EEG patients and in normal subjects investigated by fMRI evidence a significant spatial congruence in the networks of activations revealed by the two techniques [Brovelli et al., 2005]. On the other hand, the same perceptual and motor processes have frequently been associated with energy suppressions—or desynchronization—in the alpha and beta bands [Pfurtscheller, 2001] though the anatomical localization of these energy modulations did not match so neatly our knowledge of cortical functional anatomy (such as the spatial mapping of the motor cortex "homunculus" [Crone et al., 1998b]).

Taken together, these observations strongly suggest that a close anatomical correspondence may indeed exist between activation networks revealed by fMRI and EEG gamma band responses. A recent study even postulated a formal mechanism relating the phenomena measured by the two techniques [Niessing et al., 2005]: local gamma band energy modulations would require the synchronizing action of inhibitory interneurons, whose activity would substantially contribute to local oxygen consumption.

Ideally, the putative relationship between BOLD and gamma band signals should be further tested, not only in animals, but also in humans. So far, animal studies have only addressed this relationship for extremely simple cognitive processes (under anesthesia in most designs,), exclusively in the visual cortex. Yet gamma band activations are exquisitely variable across individuals, brain regions, experimental paradigms and vigilance levels [Engel et al., 1999; Fell et al., 2003; Fries et al., 2001]. Therefore and given that the primary use of fMRI is the investigation of human cognition, the putative relationship between fMRI and gamma band EEG activity should also be tested for human subjects under multiple cognitive situations—with combined fMRI and EEG recordings sampling distributed brain regions.

Intracerebral EEG recordings from patients with intractable epilepsy offer a unique vista to record electrophysiological activity in restricted human brain regions with a spatial precision equivalent to that of fMRI. While at present, intracranial recordings cannot be made simultaneously with fMRI, for safety, ethical and legal reasons, it is nonetheless possible to record the same patients with both techniques and in the same cognitive paradigms in a couple of days. To our knowledge, this constitutes the most promising possibility to date for comparing EEG and fMRI signals in humans.

Thanks to the collaboration of three epileptic patients, we were able to implement precisely such an experimental design, in a reading task paradigm. For the first study of this kind, we focused on the simple question of whether BOLD variations and EEG gamma band energy modulations induced by this reading task presented compatible anatomical distributions. An explicit relationship between the two would imply that EEG recording sites with strong gamma band energy increases evidenced in a contrast between two experimental conditions, should spatially correlate with fMRI activation clusters observed in the same contrast. We tested precisely this prediction in a contrast between semantic processing versus the visual analysis of strings of characters.

MATERIALS AND METHODS

Subjects

All three patients (P1, a 17-year-old male, P2, an 18-year-old female; P3, a 20-year-old female;) suffered from drug-resistant partial epilepsy and were candidates for surgery. Because the location of the epileptic foci could not be identified by noninvasive methods, intracerebral recordings were made by means of stereotactically implanted multilead depth electrodes (stereotactic EEG, SEEG). The selection of implant sites was based on purely clinical considerations with no reference to the present experimental protocol. Written informed consent was obtained from all

patients. All three patients were right-handed (Edimburgh scale) native French speakers. Experimental EEG sessions were conducted 4 days after implantation. MRI scans evidenced left hippocampal sclerosis in P2 and P1, and left temporal antero-lateral ganglioglioma in P3. The epileptogenic zone proved to be temporal antero-mesial in P2, and temporal mesio-lateral in P3 and P1.

Electrodes Implantation

In all three patients, 13 (P1), 15 (P2) and 12 (P3) semi-rigid electrodes were implanted in the left hemisphere, dominant for language (see Supplementary Fig. S5), in different cortical areas based on the suspected locations of seizure origin. Each electrode had a diameter of 0.8 mm and comprised 10–15.2 mm long leads, 1.5 mm apart [Dixi, Besançon, France], depending on the target region (see Supplementary Fig. S5). Thus, various mesial and lateral temporal and juxta-temporal cortical areas were recorded, including sulcal cortex and insula. The electrode contacts were identified on each individual stereotaxic scheme, and then anatomically localized using the stereotaxic atlas of Talairach and Tournoux [Talairach and Tournoux, 1988]. In addition, computer-assisted matching of post-implantation CT-scan with a pre-implantation 3-D MRI (VOXIM R, IVS Solutions, Germany) provided a direct visualization of electrode contacts with respect to each patient's brain anatomy: SEEG recording sites were positioned onto the anatomical MRI which was modified to include markers in each SEEG site and then co-registered to the functional volumes of the patient, to associate each SEEG site with a specific fMRI voxel.

MR Acquisition

Functional MR imaging was performed on a 1.5 Tesla MR imager (Philips NT) equipped with echo-planar (EPI) acquisition. Twenty-five adjacent, axial slices (thickness 5 mm each) were imaged sequentially. For each subject, only one functional scan was acquired during each fMRI session. The imaging volume was oriented parallel to the bicommissural plane. Positioning of the image planes was performed on scout images acquired in the sagital plane. An EPI MR pulse sequence was used. The main MR acquisition parameters of this sequence were: TR = 2770 ms, TE = 45 ms, flip angle = 90°, acquisition time per slice = 37 ms, field-of-view = 256 × 256 mm^2, imaging matrix = 64 × 64, reconstruction matrix = 128 × 128, total scan duration = 14 min and 46 s. Subsequent to the functional scan, a high resolution 3D anatomical MR scan was obtained from the volume examined during functional scans acquisition. The fMRi sessions were conducted before the SEEG sessions in one patient (P3), and after the SEEG sessions in the other two (P1 and P2).

Task and Stimuli

The electrodes' position in peri-sylvian cortex of the dominant hemisphere motivated the choice of a language task. The paradigm was intended to involve high-level cognitive processes unique to humans and well-documented with fMRI. The patients were recorded in three different conditions: two orthographic and visual tasks (VISUAL) and (SYMBOL) and one semantic task (SEMANTIC). In the VISUAL condition, subjects were shown a series of five- or six-letter consonant strings incongruent with French language graphotactic rules (i.e. "xwxqn") and their task was to identify whether the string contained twice the same character. In the SYMBOL condition, the conditions and the task were identical except that the letters were replaced by unreadable symbols, unknown to the subjects white *Karalyn Pattersen* false font characters (examples of which can be seen in (Price, 2000)). As data analysis revealed no differences between the VISUAL and SYMBOL conditions, both were fused into the CONTROL task. In the SEMANTIC task, subjects were asked to judge whether five or six letters words represented living entities or not.

A "block" design was used which alternated nine periods, each one composed of three epochs (VISUAL, SYMBOL and SEMAN epochs), the order of which was varied pseudo-randomly between blocks. Each epoch lasted 1 min and comprised of 20 stimuli.

All stimuli were presented foveally on a 17″ computer screen, as black lower-case letters on a white background (courier font, size 35 mm). Between stimuli, a black crosshair (size 35 mm) was presented in the center of the screen. Stimuli were presented for durations of 2 s each with a random interstimuli intervals ranging between 2,800 and 3,200 ms. The patients were instructed to respond by pressing a manual key with the index finger of their left hand. Stimuli were generated by means of Psyscope V.1.1 (Carnegie Mellon Department of Psychology) running on a Macintosh computer (Power Macintosh 9600). They were shown to subjects inside the magnet by means of a video projector (*Eiki LC* 6000), a projection screen situated behind the magnet and a mirror centred above the subject's eyes.

EEG Data Analysis

Intracerebral recordings were conducted using an audio-video-EEG monitoring system (Micromed, Treviso, Italy), which allowed the simultaneous recording of 63 depth-EEG channels sampled at 512 Hz [0.1–200 Hz bandwidth]. Recording sites showing clear epileptiform activities were excluded from the analysis, and among the remaining sites, monopolar and bipolar data were systematically inspected, both raw and high-pass filtered (above 15 Hz), and any trial showing epileptic spikes in any of those traces was discarded. Note that high-pass filtering was used only for artifact detection, all the analyses were performed on raw unfiltered data.

Time-Frequency Analysis

EEG signals were evaluated with the software package for electrophysiological analysis (ELAN-Pack) developed at the INSERM U280 laboratory. For each single trial, bipolar derivations computed between adjacent electrode contacts were analyzed in the time-frequency domain by convolution with complex Gaussian Morlet's wavelets, thus providing a time-frequency power map $P(t,f) = |w(t,f) \times s(t)|^2$, where $w(t,f)$ was for each time t and frequency f a complex Morlet's wavelet $w(t,f) = A \exp(-t^2/2\sigma_t^2)\exp(2i\pi ft)$, with $A = (\sigma_t\sqrt{\pi})^{-1/2}$ and $\sigma_t = 1/(2\pi\sigma_f)$ and σ_f a function of the frequency f: $\sigma_f = f/7$ (Tallon-Baudry et al., 1996).

Normalized time-frequency maps were computed for each bipolar derivation, for visualization purpose. This normalization was done separately for each frequency, and consisted in (a) subtracting the mean power during a [−500 ms:−100 ms] prestimulus baseline and (b) dividing by the standard deviation of the power during this same baseline.

Comparison between conditions (SEMANTIC vs. CONTROL) were done via a Mann-Whitney non-parametric analysis applied on the raw time-frequency values of energy, on a set of time-frequency tiles [80 ms × 8 Hz] covering a [−500:2500 ms] × [1:200 Hz] domain with an overlap of 50% along both time and frequency axis (one test per tile comparing the values obtained for all the trials in the two conditions). The results of this analysis are time-frequency maps indicating TF domains in which EEG energy is significantly different between the two conditions; those maps were used to directly estimate the duration of those effects in the gamma band.

fMRI Data Analysis

The functional data were pre-processed with SPM2 software (http://www.fil.ion.ucl.ac.uk/spm/) implemented in Matlab (The Mathworks, Inc.). The analysis was performed independently on each patient. fMRI data were first (a) realigned to a scan recorded halfway within the time series for motion correction and (b) spatially smoothed in the x,y direction (Gaussian kernel, 6 mm half-width). The first two scans within a block were discarded to avoid modelling of the haemodynamic response and the global activity in each scan was corrected by grand mean scaling. Functional data analysis used a General Linear Model using the conditions as factors of interest and the runs as confounds to compute parameter estimates. Since the two conditions "consonant strings" and "Karalyn Pattersen" were pooled together into a single control condition, the result was finally expressed by the contrast (named "semantic-control") 2*"word" -("consonant strings" + "Karalyn Pattersen") and by the P value corresponding to the comparison of this contrast to zero at each voxel. Those P values are indicated in the figures for each patient.

RESULTS AND DISCUSSION

As announced in the introduction, our objective was to determine whether fMRI, taken in isolation, has any predictive value about the anatomical location of cross-condition gamma band modulations. Following our starting hypothesis that gamma band energy modulations impose local haemodynamic signals variations, a logical prediction was that in the SEMANTIC–CONTROL contrast, at least one BOLD activation cluster should be found in the immediate vicinity of each EEG recording site showing differences in gamma band energy in the same contrast. Testing this prediction implied first, identifying EEG sites with a significant cross-conditions difference in gamma band energy, and second, estimating the distance between such sites and the closest BOLD activation cluster (anatomical locations of which can be found in Supplementary Tables I, II and III).

TABLE I. Precise anatomical location of the sites with a significant difference in gamma band energy between the two experimental conditions[a]

Patient	Site	x	y	z	Location
P1	U′6	−53	−26	11	Superior temporal gyrus, posterior part (BA42)
P1	U′7	−56	−26	11	Superior temporal gyrus, posterior part (BA42)
P1	U′8	−59	−26	11	Superior temporal gyrus, posterior part (BA42)
P1	U′9	−63	−26	11	Superior temporal gyrus, posterior part (BA42)
P1	Y′14	−22	44	18	Inferior frontal gyrus, rostral part (BA46)
P2	S′9	−58	−11	18	Post-central operculum (BA43)
P2	Q′7	−51	12	9	Inferior frontal gyrus, caudal part (BA44)
P2	G′11	−42	38	12	Inferior frontal gyrus, rostral part (BA45/46)
P3	U′2	−36	−42	12	Superior temporal gyrus, posterior part (BA22)
P3	U′3	−40	−42	12	Superior temporal gyrus, posterior part (BA22)
P3	U′6	−50	−42	12	Superior temporal gyrus, posterior part (BA22)
P3	U′9	−60	−42	12	Superior temporal gyrus, posterior part (BA22)
P3	T′10	−60	−48	16	Superior temporal gyrus, posterior part (BA22)
P3	F′2	−25	−51	−9	Lingual gyrus (BA37/19)
P3	V′15	−56	−60	21	Supra-marginalis gyrus (BA39/40)

[a] Selected using the criterion defined in Figure 1; x, y, and z are the Talairach coordinates of the sites in millimeters.

EEG time-frequency analysis revealed strong statistical differences between semantic and control conditions in frequencies above 40 Hz, i.e. in the gamma band. Yet, those differences across conditions occurred only in a small subset of the recording sites (15 out of 89). In those 15 sites, hereafter referred to as "gamma sites" (see Table I), the modulations were characterized by their wide frequency extent (typically up to 150 Hz) and their duration: the statistical difference lasting at least 100 ms in the [40–150 Hz] band (see Fig. 1a). Figure 2 and Supplementary Figures S1 and S3 show for each patient time-frequency maps for gamma sites in both CONTROL and SEMANTIC conditions, in relation to their fMRI activation maps in the SEMANTIC–CONTROL contrast.

Next, we measured the distance separating each of those gamma sites from its nearest fMRI activation cluster (activation clusters being defined as sets of contiguous voxels above the significance threshold in the SEMANTIC–CONTROL contrast, see methods). This analysis revealed that 12 out of the 15 (80%) gamma sites were located <15 mm away from an fMRI activation cluster, which corresponds to an anatomical separation of a voxel or less (Fig. 1b). In comparison, 35 out of the 74 (47%) non-gamma sites were <15 mm away from an fMRI activation cluster. To test statistically the hypothesis that the 12 "close gamma sites" were closer to fMRI activation clusters than the other 77 sites (the three remaining and "distant" gamma sites receive our special attention in the next paragraph), we designed a simple randomization test consisting in (a) forming for each patient a *target* group with the subset of the 12 gamma sites corresponding to their implantation and 1,000 *surrogate* groups of similar size randomly drawn from all the recorded sites within each group, and (b) calculating the average distance separating a site from its nearest BOLD cluster. This procedure showed that for all three patients, this average distance was significantly smaller for the target group than for the surrogate groups (P1: smaller than 0.002% of the surrogate groups ($P = 2 \times 10^{-5}$). P2: $P = 1.2 \times 10^{-3}$; P3: $P = 2.9 \times 10^{-3}$).

A closer investigation of the three "distant" gamma sites revealed that although they displayed an initial, and transient, superiority effect for the SEMANTIC condition, they were also characterized by a later inversion of this effect, with a stronger gamma energy for the CONTROL condition after 500–700 ms (see Figs. 2 and 3; Supplementary Figs. S1 and S2 for statistical maps). Such effects reversals caused the total gamma energy during the whole response window to be equivalent in the two conditions or even slightly higher for the CONTROL condition. This may explain why they did not correspond to any activation in the fMRI SEMANTIC–CONTROL, given the fact that fMRI slices were acquired every 3 s. We wish to highlight those three examples as they illustrate potentially meaningful differences in neural activations which can only be revealed by time-resolved neural recordings.

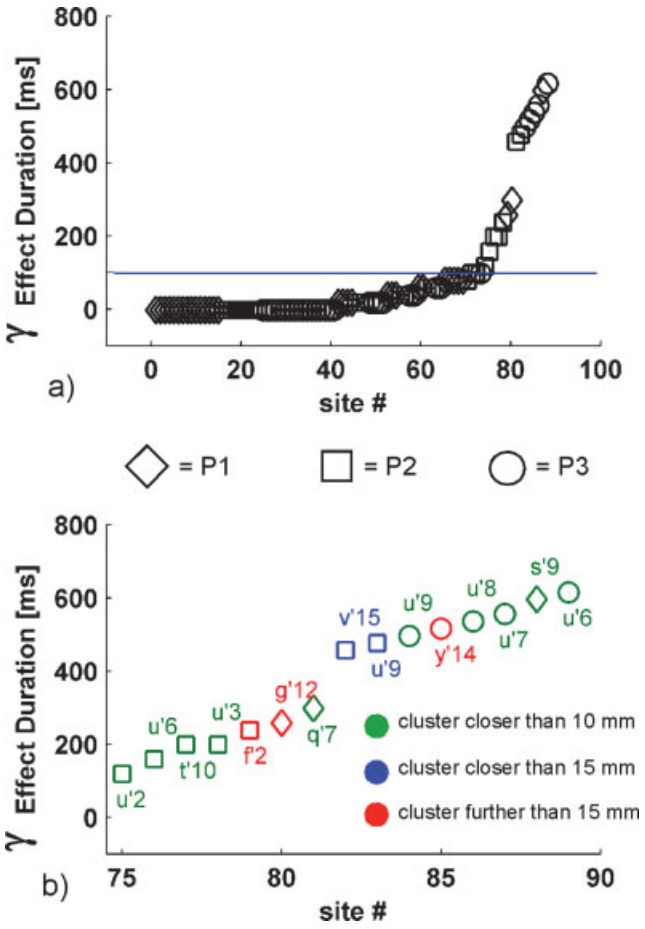

Figure 1.

Spatial relationship between BOLD and SEEG gamma modulations. (**a**) Maximal duration of significant energy difference between the SEMANTIC and the CONTROL conditions in the [40–150 Hz] band, for all the EEG sites. For each site, this value corresponds to the duration of the longest time window, across all frequencies in the gamma band, during which the *P*-value for the Mann-Whitney comparison between the two conditions stays lower than 1×10^{-4}. Sites for which this duration exceeds 100 ms are referred to as "gamma sites" in the text. The markers shapes indicate which patient was recorded; (**b**) same for the 15 sites for which the maximal duration is longer than 100 ms. Sites closer than 10 mm (resp. 15 mm) away from a fMRI activation cluster (i.e. sets of contiguous voxels above the significance threshold) in the SEMANTIC–CONTROL are shown in green (resp. blue), the remaining sites are shown in red. [Color figure can be viewed in the online issue, which is available at www.interscience.wiley.com.]

In addition to the SEMANTIC–CONTROL contrast, we also tested whether the reverse CONTROL–SEMANTIC contrast would reveal brain regions with stronger BOLD signal in the control condition and how those regions would respond in the gamma band (Fig. S6). There were

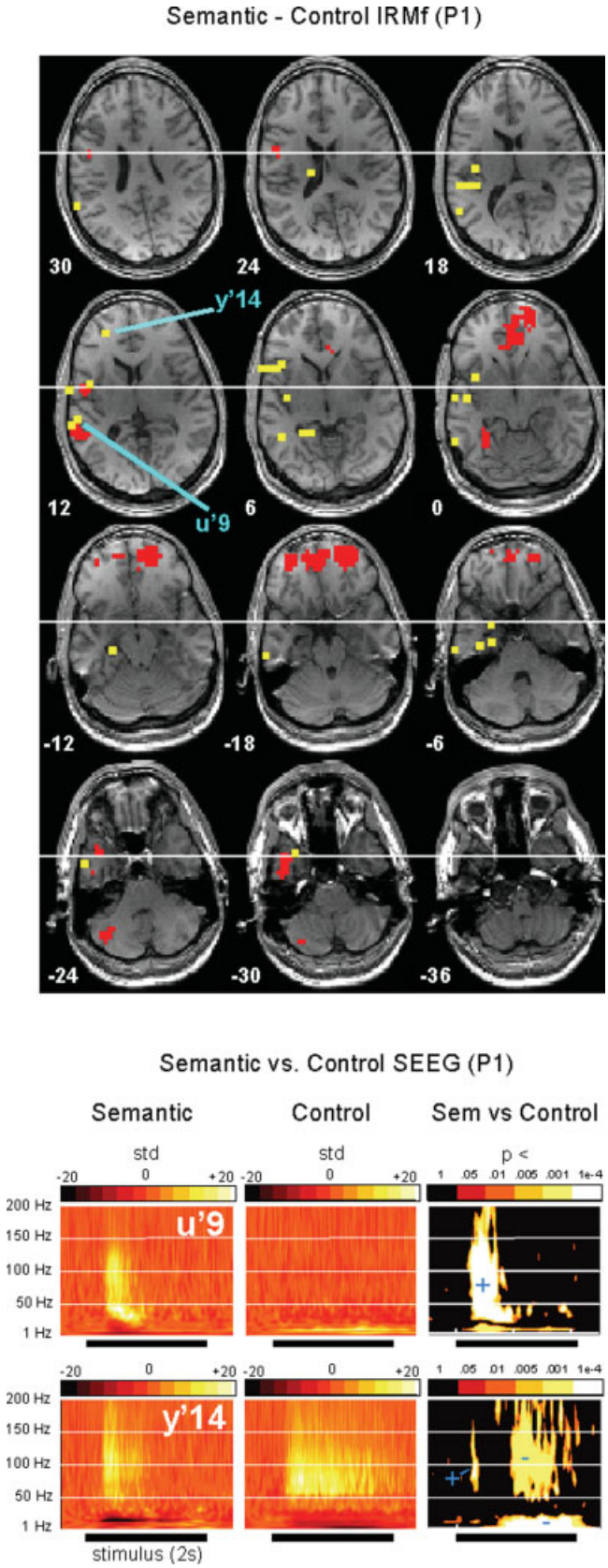

indeed such effects in all three patients, predominantly in the visual cortex, which was expected since the control task required detailed visual inspection of the character strings. Except in patient P3, there were no EEG recording sites in the vicinity of those negative BOLD responses (<15 mm). In patient P3, three recording sites were located <15 mm from negative BOLD clusters (see Fig. S6), however, no significant differences were found between conditions.

The previous examples do not disprove the suspected relationship between BOLD signals and gamma band activations: altogether, our analysis showed that sites with a gamma energy increase globally stronger in the SEMANTIC–CONTROL contrast were significantly closer than the other sites to fMRI activation clusters revealed in the same contrast. This implies that fMRI could be used, in this particular experimental situation, as a spatial predictor of such gamma modulations; that is, fMRI could indicate cortical regions where sites with a stronger gamma band response in the semantic condition would be more likely to be found.

However, this predictive power should not be understood in the strong sense that any SEEG site in the vicinity of a fMRI cluster should record task-related gamma modulations. While significant gamma band modulations were observed in the vicinity of fMRI activation clusters, the converse was in general not true. This was expected because depth electrodes sample only restricted portions of the volumes surrounding the fMRI activation clusters:

Figure 2.

Semantic–Control contrasts in fMRI and SEEG (patient P1). The top panel shows the fMRI images of statistically significant increases in BOLD signal from the CONTROL to the SEMANTIC condition (red voxels), thresholded at $P < 0.001$, superimposed on transverse sections of P1's brain. Yellow dots indicate the brain sites recorded in SEEG, while blue lines point at sites U'9 and Y'14 where task-related EEG modulations longer than 100 ms were observed in the [40–150 Hz] band. The bottom panels show for each of those sites the time-frequency maps in the two conditions (left and middle maps, each time-course is expressed in units of the standard deviation of the [−500:−100 ms] prestimulus period). Time-frequency maps on the right show the *P*-values of a Mann-Whitney comparison between the SEMANTIC and CONTROL conditions. Regions where the SEMANTIC (resp. CONTROL) condition dominates are indicated by a blue plus (resp. minus) sign. U'9, shows a clear superiority effect of the SEMANTIC condition and is adjacent to a fMRI activation cluster, in the posterior part of the superior temporal gyrus. Y'14, in the inferior frontal gyrus, is >15 mm away from the nearest BOLD cluster, but the effect there is ambiguous: the gamma energy is initially stronger for the semantic condition, before the effect reverses after 500 ms. See the supplementary materials for a similar figure for the other two patients. [Color figure can be viewed in the online issue, which is available at www.interscience.wiley.com.]

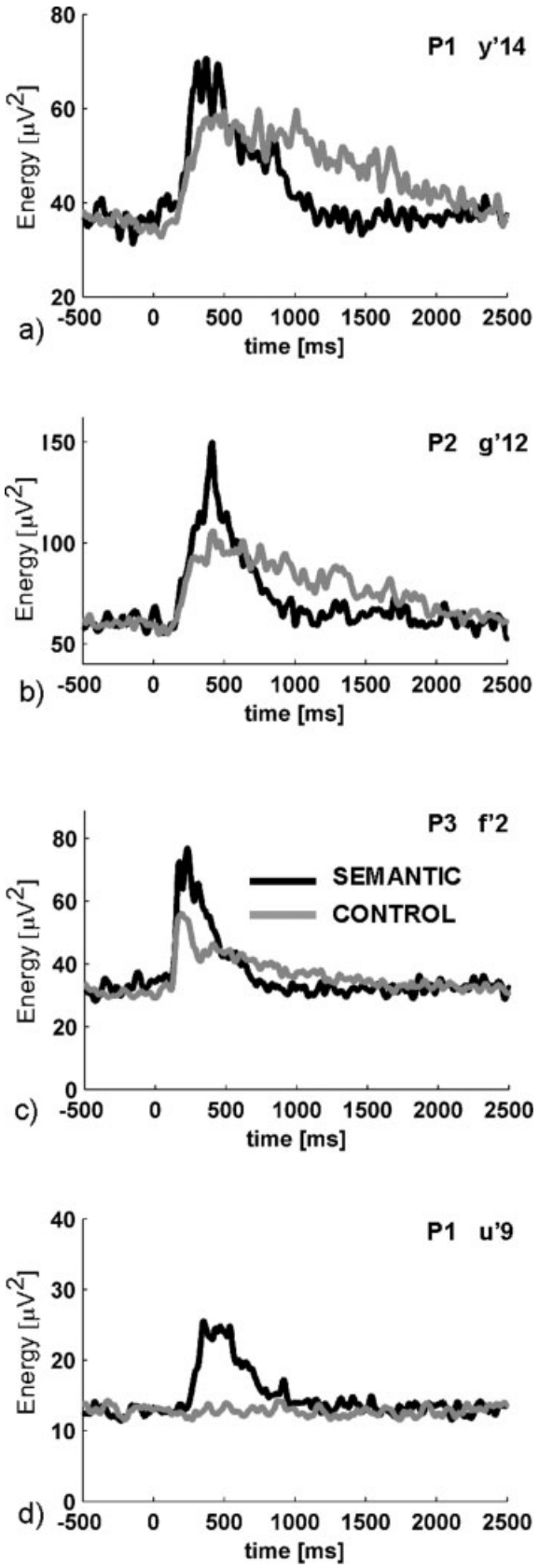

gamma modulations were very focal (see Fig. S4, supplementary materials), and it follows that the presence of an fMRI activation cluster in a brain region may imply a local increase of gamma energy somewhere in its surrounding, without necessary involving the ignition of the entire surroundings. Indeed, Figure S4 illustrates the case of two recording sites separated by only 3.5 mm along the same electrode. Although the two sites were equally close to the nearest fMRI activation cluster, they displayed sharply different gamma modulations.

In summary, our results support the view that the functional networks revealed by fMRI are spatially congruent with the mosaic of gamma activations revealed in humans by intracranial EEG recordings. Obviously, a single study is not sufficient to prove a systematic relationship between the two phenomena, especially given the small number of patients investigated here, but this one corroborates, in maybe the most direct experimental context in humans given present safety constraints, the link already demonstrated in animal models, with their associated strengths and limitations. A definitive proof will now require a multiplicity of studies of this kind, combining fMRI and intracranial EEG in the same patients, across a wide range of brain explorations and cognitive situations, in conjunction with further animal studies. The two imaging approaches, SEEG and fMRI, appear in fact very complementary, neither of them being sufficient by itself: intracranial EEG recordings suffer from their limited sampling of the brain volume, while fMRI is ill-suited to distinguishing between activations with similar global energy but different time courses. Altogether, this study encourages further research efforts to combine fMRI, either with intracerebral EEG, or scalp EEG (and MEG) through source-reconstruction algorithms.

ACKNOWLEDGMENTS

The authors thank Valérie Balle, Patricia Boschetti, Carole Chatelard, Véronique Dorlin, Eliane Gamblin, and Martine Juillard for their invaluable technical help; and Benjamin Schoendorff and Karim Jerbi for their precious comments on the manuscript. J.-P.L. was supported by a grant from the Fyssen Fundation.

Figure 3.

Biphasic energy modulations in the gamma band. Each graph shows the mean energy profile in the [40–150 Hz] frequency band for the CONTROL (gray) and SEMANTIC (black) conditions. (**a**,**b**,**c**) correspond to the only sites with a clear condition-effect in the gamma band which are far (>15 mm) from a BOLD contrast cluster. In all three cases, the initial burst of gamma energy is stronger in the SEMANTIC condition, while its tail is stronger in the CONTROL condition. Such effects, which may be frequent in functional imaging studies, are problematic for fMRI. (**d**) shows an unambiguous semantic superiority effect for comparison.

REFERENCES

Aoki F, Fetz EE, Shupe L, Lettich E, Ojemann GA (2001): Changes in power and coherence of brain activity in human sensorimotor cortex during performance of visuomotor tasks. Biosystems 63:89–99.

Brovelli A, Lachaux JP, Kahane P, Boussaoud D (2005): High gamma frequency oscillatory activity dissociates attention from intention in the human premotor cortex. Neuroimage 28:154–164.

Crone NE, Miglioretti DL, Gordon B, Lesser RP (1998a): Functional mapping of human sensorimotor cortex with electrocorticographic spectral analysis. II. Event-related synchronization in the gamma band. Brain 121 (Part 12):2301–2315.

Crone NE, Miglioretti DL, Gordon B, Sieracki JM, Wilson MT, Uematsu S, Lesser RP (1998b): Functional mapping of human sensorimotor cortex with electrocorticographic spectral analysis. I. α and β event-related desynchronization. Brain 121 (Part 12):2271–2299.

Engel AK, Fries P, Konig P, Brecht M, Singer W (1999): Temporal binding, binocular rivalry, and consciousness. Conscious Cogn 8:128–151.

Fell J, Klaver P, Lehnertz K, Grunwald T, Schaller C, Elger CE, Fernandez G (2001): Human memory formation is accompanied by rhinal-hippocampal coupling and decoupling. Nat Neurosci 4:1259–1264.

Fell J, Fernandez G, Klaver P, Elger CE, Fries P (2003): Is synchronized neuronal γ-activity relevant for selective attention? Brain Res Brain Res Rev 42:265–272.

Foucher JR, Otzenberger H, Gounot D (2003): The BOLD response and the gamma oscillations respond differently than evoked potentials: An interleaved EEG-fMRI study. BMC Neurosci 4:22.

Fries P (2005): A mechanism for cognitive dynamics: Neuronal communication through neuronal coherence. Trends Cogn Sci 9:474–480.

Fries P, Reynolds JH, Rorie AE, Desimone R (2001): Modulation of oscillatory neuronal synchronization by selective visual attention. Science 291:1560–1563.

Howard MW, Rizzuto DS, Caplan JB, Madsen JR, Lisman J, Aschenbrenner-Scheibe R, Schulze-Bonhage A, Kahana MJ (2003): Gamma oscillations correlate with working memory load in humans. Cereb Cortex 13:1369–1374.

Kayser C, Kim M, Ugurbil K, Kim DS, Konig P (2004): A comparison of haemodynamic and neural responses in cat visual cortex using complex stimuli. Cereb Cortex 14:881–891.

Kim DS, Ronen I, Olman C, Kim SG, Ugurbil K, Toth LJ (2004): Spatial relationship between neuronal activity and BOLD functional MRI. Neuroimage 21:876–885.

Klopp J, Halgren E, Marinkovic K, Nenov V (1999): Face-selective spectral changes in the human fusiform gyrus. Clin Neurophysiol 110:676–682.

Lachaux JP, Rodriguez E, Martinerie J, Adam C, Hasboun D, Varela FJ (2000): A quantitative study of gamma-band activity in human intracranial recordings triggered by visual stimuli. Eur J Neurosci 12:2608–2622.

Lachaux JP, George N, Tallon-Baudry C, Martinerie J, Hugueville L, Minotti L, Kahane P, Renault B (2005): The many faces of the gamma band response to complex visual stimuli. Neuroimage 25:491–501.

Lachaux JP, Hoffmann D, Minotti L, Berthoz A, Kahane P (2006): Intracerebral dynamics of saccade generation in the human frontal eye field and supplementary eye field. Neuroimage 30:1302–1312.

Logothetis NK, Pauls J, Augath M, Trinath T, Oeltermann A (2001): Neurophysiological investigation of the basis of the fMRI signal. Nature 412:150–157.

Mainy N, Kahane P, Minotti L, Hoffmann D, Bertrand O, Lachaux JP (2006): Neural correlates of consolidation in working memory. Hum Brain Mapp.

Niessing J, Ebisch B, Schmidt KE, Niessing M, Singer W, Galuske RA (2005): Haemodynamic signals correlate tightly with synchronized gamma oscillations. Science 309:948–951.

Pfurtscheller G (2001): Functional brain imaging based on ERD/ERS. Vision Res 41:1257–1260.

Price CJ (2000): The anatomy of language: Contributions from functional neuroimaging. J Anat 197 (Part 3):335–359.

Singer W (1999): Neuronal synchrony: A versatile code for the definition of relations? Neuron 24:49–65. 111–125.

Szurhaj W, Bourriez JL, Kahane P, Chauvel P, Mauguiere F, Derambure P (2005): Intracerebral study of gamma rhythm reactivity in the sensorimotor cortex. Eur J Neurosci 21:1223–1235.

Talairach J, Tournoux P. (1988). Co-Planar Stereotaxic Atlas of the Human Brain. 3-Dimensional Proportional System: An Approach to Cerebral Imaging. New York: Thieme.

Tallon-Baudry C, Bertrand O, Delpuech C, Pernier J (1996): Stimulus specificity of phase-locked and non-phase-locked 40 Hz visual responses in human. J Neurosci 16:4240–4249.

Tallon-Baudry C, Bertrand O, Fischer C (2001): Oscillatory synchrony between human extrastriate areas during visual short-term memory maintenance. J Neurosci 21:RC177.

Tallon-Baudry C, Bertrand O, Henaff MA, Isnard J, Fischer C (2005): Attention modulates gamma-band oscillations differently in the human lateral occipital cortex and fusiform gyrus. Cereb Cortex 15:654–662.

Tanji K, Suzuki K, Delorme A, Shamoto H, Nakasato N (2005): High-frequency gamma-band activity in the basal temporal cortex during picture-naming and lexical-decision tasks. J Neurosci 25:3287–3293.

Varela F, Lachaux JP, Rodriguez E, Martinerie J (2001): The brainweb: Phase synchronization and large-scale integration. Nat Rev Neurosci 2:229–239.